Article

miR193a-5p Mediated ZNF746 and c-Myc Signaling Axis Is Critically Involved in Morusin Induced Apoptosis in Colorectal Cancer Cells

Woon-Yi Park, Hyo-Jung Lee, Deok-Yong Sim, Eunji Im, Ji-Eon Park, Chi-Hoon Ahn, Bum-Sang Shim * and Sung-Hoon Kim *

Department of Korean Pathology, College of Korean Medicine, Kyung Hee University, Seoul 02447, Korea; wy1319@naver.com (W.-Y.P.); hyonice77@naver.com (H.-J.L.); simdy0821@naver.com (D.-Y.S.); ji4137@naver.com (E.I.); wdnk77@naver.com (J.-E.P.); ach2565@naver.com (C.-H.A.)

* Correspondence: eshimbs@khu.ac.kr (B.-S.S.); sungkim7@khu.ac.kr (S.-H.K.); Tel.: +82-2-961-9233 (S.-H.K.)

Abstract: Novel target therapy is on the spotlight for effective cancer therapy. Hence, in the present study, the underlying apoptotic mechanism of Morusin was explored in association with miR193a-5p mediated ZNF746/c-Myc signaling axis in colorectal cancer cells (CRCs). Herein, Morusin reduced the viability and the number of colonies in HCT116 and SW480 CRCs. Additionally, Morusin increased sub-G1 population, cleavages of poly (ADP-ribose) polymerase (PARP) and caspase-3 and inhibited the expression of zinc finger protein 746 (ZNF746) and c-Myc in HCT116 and SW480 cells. Conversely, overexpression of ZNF746 suppressed the ability of Morusin to abrogate the expression of c-Myc in HCT116 cells, as ZNF746 enhanced the stability of c-Myc via their direct binding through nuclear colocalization in HCT116 cells by immunofluorescence and immunoprecipitation. Notably, Morusin upregulated miR193a-5p as a tumor suppressor, while miR193a-5p inhibitor masked the ability of Morusin to reduce the expression of ZNF746, c-Myc, and pro-PARP in HCT116 cells. To our knowledge, these findings provide the novel insight on miR193a-5p mediated inhibition of ZNF746/c-Myc signaling in Morusin induced apoptosis in CRCs.

Keywords: morusin; colorectal cancer; apoptosis; ZNF746/c-Myc; miR-193a-5p

1. Introduction

Colorectal cancer (CRC) is reported as the fourth most prevalent cancer in women and the third most common cancer in men worldwide [1,2]. Despite modern medicine, approximately 50% of CRC patients have experienced tumor recurrence, and their overall mortality rate is estimated up to approximately 40% [3]. Though chemotherapy, mainly with 5-FU, oxaliplatin (FOLFOX), Irinotecan and Cetuximab, radiotherapy and surgery. have been utilized for CRC treatment for years, recently molecular target therapy is of interest for EGFR, RAS, and VEGF [4,5].

It is well documented that c-Myc is a biomarker for poor prognosis of CRC patients, as it is a transcription factor that is critically associated with cell growth, cell adhesion, proliferation, and apoptosis [6]. Hence, to target c-Myc has been considered a good strategy for prevention or treatment of CRCs [7]. Additionally, ZNF746, with a C2HC/C2H2 type zinc finger protein at its C terminus [8,9] and a Kruppel-associated box at its N terminus [10,11], is known to act as a suppressor of PPAR gamma [12], regulate Parkin as a ubiquitin E3 ligase [13], and enhance the stability of c-Myc [1]. Additionally, accumulating evidence reveals that many miRNAs are critically involved in cancer biology as oncogenes or tumor suppressors [14–16].

Additionally, some natural compounds such as quercetin [17], ursolic acid [18], and curcumin [19] are being considered for combination therapy with classical anticancer agents. In the same line, Morusin, one of the prenylated flavonoids [20–22] derived from

the root bark of *Morus alba*, is known to have anti-microbial [23], anti-inflammatory [24], and antitumor [3,25,26] effects. Nonetheless, its underlying molecular mechanism remains unclear in CRCs to date. Thus, in the present study, the molecular mechanism of Morusin was explored in CRCs, targeting c-Myc and ZNF746 signaling mediated by miRNA 193a-5p as a tumor suppressor.

2. Materials and Methods

2.1. Cell Culture

Human colorectal HCT116 (ATCC® CCL-247), SW480 (ATCC® CCL-228) cancer cell lines supplied from American Type Culture Collection (ATCC) were maintained in RPMI1640 with 1% antibiotic and 10% FBS (Welgene, Gyeongsan, Korea) in Forma 320 CO_2 incubator (Marshal Scientific Company, Hampton, NH, USA). All experiments were conducted in the 75–80% confluence of the cells.

2.2. Cell Viability Assay

Based on Jung et al.'s paper [1], cell viability assay was conducted in HCT116 and SW480 CRCs by using MTT assay. Briefly, HCT116 and SW480 cells (1×10^4 cells/well) were exposed to Morusin (0, 2.5, 5, and 10 μM) for 24 h and incubated with MTT (1 mg/mL) (Sigma-Aldrich, Saint Louis, MO, USA) for 2 h. The viability was calculated with optical density (OD) values as a percentage of viable cells in Morusin treated group versus untreated control. All assays were conducted in independent triplicates.

2.3. Colony Formation Assay

HCT116 and SW480 cells (3×10^3/well) exposed to Morusin (0, 2.5, and 5 μM) for 24 h were distributed onto 6-well plates for a week. The cells were washed PBS, fixed, and stained with Diff quick solution (Sysmex, Kobe, Japan). Then, the colonies were counted under inverted microscope.

2.4. Cell Cycle Analysis

HCT116 and SW480 cells (2×10^5 cells/mL) exposed to Morusin (0, 2.5, or 5 μM) for 24 h were incubated with RNase A (10 mg/mL) for 1 h at 37 °C and stained with propidium iodide (50 μg/mL) in dark. The stained cells were analyzed for the DNA content by FACS Calibur with CellQuest Software.

2.5. Cycloheximide Assay

HCT116 and SW480 cells treated by Morusin (5 μM) for 24 h were exposed to 50 μg/mL cycloheximide for various times (0, 15, 30, and 60 min) before Western blotting.

2.6. Western Blotting

Based on Kim et al.'s paper [12], HCT116 and SW480 cells (1×10^6 cells/mL) were exposed to Morusin (0, 2.5, or 5 μM) of for 24 h, The supernatants were collected and quantified for protein concentration by using RC DC protein assay kit (Bio-Rad, Hercules, CA, USA), The protein samples (30 μg of protein from cells) were separated on 4–12% NuPAGE Bis–Tris gels (Novex, Carlsbad, CA, USA) and ECL transfer membrane for detection with antibodies for PARP (#9542), pro-caspase-3 (#9662), cleaved caspase-3 (#9664), c-Myc (Y69) and ZNF746 (LS-B8045), Bcl-2 (SC-492), Bcl-xL (SC-8392), and β-actin (A2228) (Sigma, St. Louis, MO, USA). Proteins were detected using the ECL system (Amersham Pharmacia Biotech INC, District of Columbia, MO, USA). Densitometric analysis was performed using ImageJ software.

2.7. TUNEL Assay

Based on Park et al.'s paper [6], to detect cell death, HCT116 or SW480 cells were treated with Morusin (5 μM) for 24 h, and incubated with TUNEL assay mixture for 60 min by using the DeadEnd™ Fluorometric TUNEL system kit (Promega, Madison, WI, USA).

Then, TUNEL-stained cells were visualized by a Delta Vision imaging system (Applied Precision, Issaquah, WA, USA).

2.8. RT-qPCR Analysis

Based on Jung et al.'s paper [1], total RNA from HCT116 cells exposed to Morusin (5 μM) was isolated by QIAzol (Invitrogen, Carlsbad, CA, USA) and synthesized with oligo dT (Bioneer, Daejeon, Korea) and M-MLV reverse transcriptase (Enzynomics, Daejeon, Korea), followed by qRT-PCR analysis by using Light cyclerTM (Roche, Basel, Switzerland) for miR193a-5p.

2.9. RNA Interference

HCT116 cells were transfected with miR-193a-5p mimic, miR-193a-5p inhibitor Sequence (5'-3'):UGGGUCUUUGCGGGCGAGAUGA, miR-Con, and miR-Con inhibitor (200 nM) (Bioneer, Daejeon, Korea), or Flag-ZNF746 plasmids by using X-tremeGENE HP DNA Transfection Reagent (Roche, Basel, Switzerland) for next experiments.

2.10. Co-Immunoprecipitation

HCT116 cells exposed to Morusin (5 μM) for 24 h were lyzed in lysis buffer and immunoprecipitated with ZNF746 antibody or normal immunoglobulin G antibody, then protein A/G sepharose beads (Santa Cruz Biotechnology, Santa Cruz, CA, USA). The precipitated proteins were subjected to immunoblotting with the antibodies of ZNF746 and c-Myc.

2.11. Immunofluorescence

HCT116 cells exposed to Morusin (5 μM) for 24 h were fixed with 4% formaldehyde and then permeabilized in 0.1% Triton X-100. The fixed cells were incubated with primary antibodies of ZNF746, c-Myc (Cell signaling, Boston, MA, USA) and then incubated with Alexa Fluor 546 goat rabbit-IgG antibody (Life technologies, Waltham, MA, USA) (1:1000) for 1 h. Finally, the nuclei of the cells stained with DAPI (Sigma, Saint Louis, MO, USA) were photographed for images of ZNF746, c-Myc, and DAPI by a Delta Vision imaging system (Applied Precision, Issaquah, WA, USA).

2.12. Statistical Analysis

All data represent means ± standard deviation (SD). For statistical analysis Student's *t*-test was used for comparison of two groups by using GraphPad Prism software (Version 5.0, CA, USA). The statistical significance was determined at *p* value of < 0.05 between control and Morusin treated groups.

3. Results

3.1. Cytotoxic Effect of Morusin in Colorectal Cancer Cells

To explore the cytotoxic effect of Morusin (Figure 1A), a cell viability assay was carried out in HCT116 and SW480 CRCs by MTT assay. The cells were exposed to Morusin (0, 2.5, 5, and 10 μM) for 24 h. Here, Morusin inhibited the viability in HCT116 and SW480 cells (Figure 1B), while HCT116 cells were more susceptible to Morusin compared to SW480 cells. Likewise, Morusin reduced the number of colonies in HCT116 and SW480 cells by the colony formation assay (Figure 1C).

3.2. Morusin Induced Apoptosis in HCT116 and SW480 Cells

To confirm the apoptotic effect of Morusin, cell cycle assay and Western blotting were conducted in Morusin treated HCT116 and SW480 cells. Herein, Morusin increased sub-G1 population in HCT116 and SW480 cells compared to untreated control (Figure 2A,B). Consistently, Morusin enhanced the cleavage of PARP, and reduced the expression of pro-PARP and pro-caspase 3 in HCT116 and SW480 cells (Figure 2C,D).
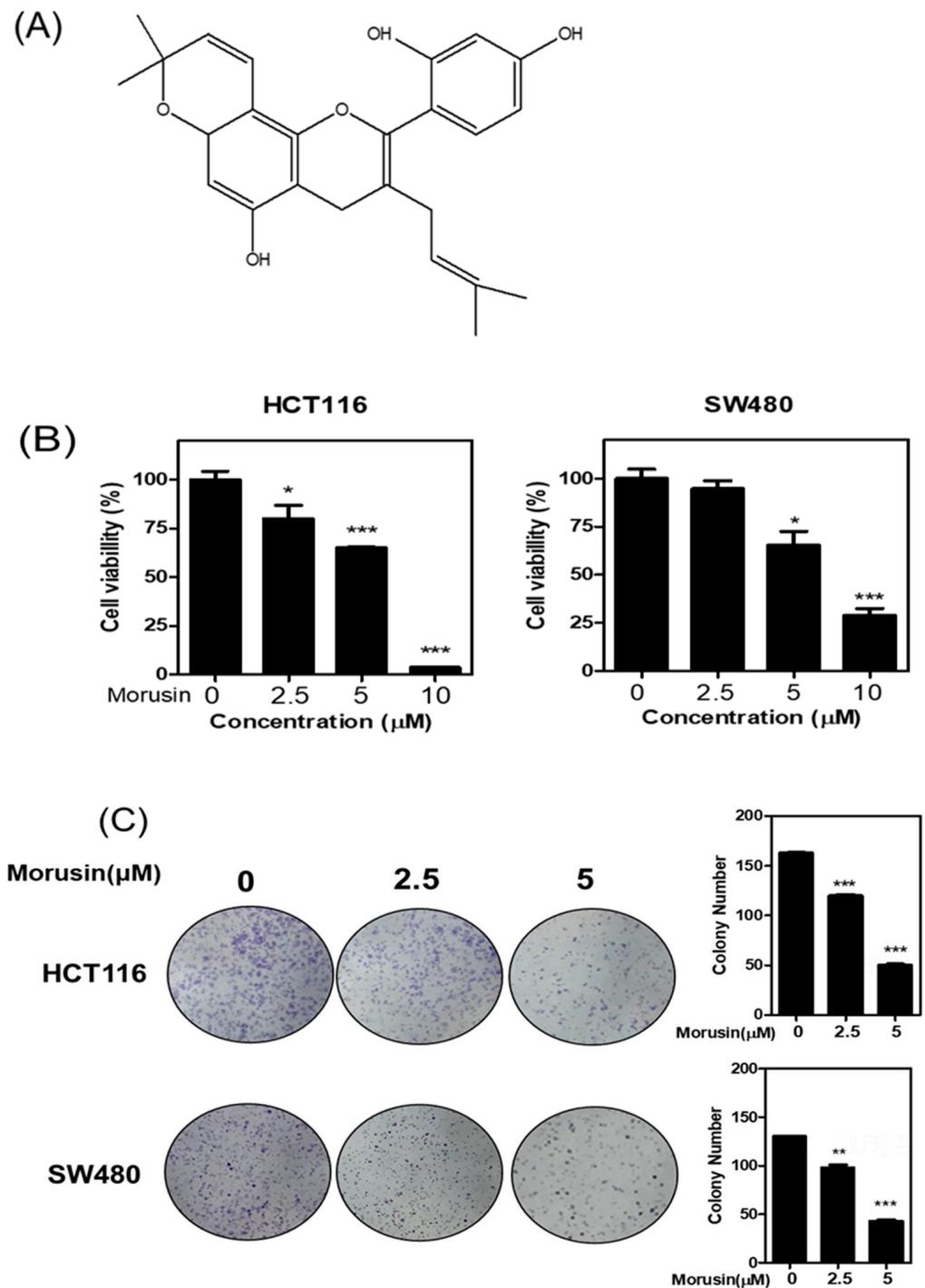
Figure 1. Effect of Morusin on cytotoxicity in HCT116 and SW480 cells. (**A**) Chemical structure of Morusin. (**B**) HCT116 and SW480 cells were exposed to various concentrations of Morusin (0, 2.5, 5, and 10 μM) for 24 h and cell viability was evaluated by MTT assay. Data stand for means ± SD of three independent experiments. * $p < 0.05$, ** $p < 0.01$ versus untreated control. (**C**) Photos for colony formation of Morusin (0, 2.5, and 5 μM) treated HCT116 and SW480 cells. The colonies were visualized by staining with Diff-Quick solution (Sysmex, Japan). Data represent means ± SD of three independent experiments. * $p < 0.05$, ** $p < 0.01$, *** $p < 0.001$ versus untreated control.
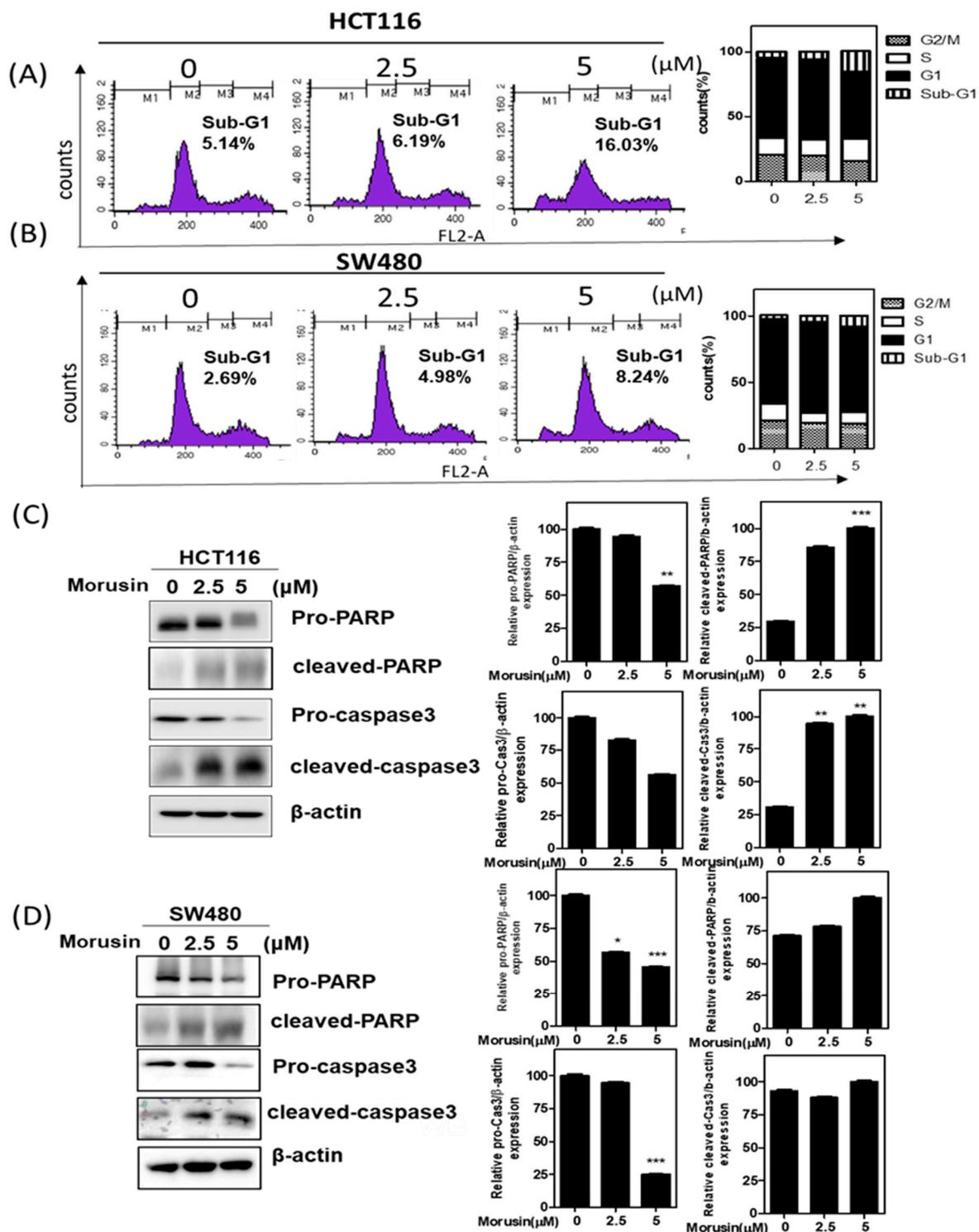
Figure 2. Effect of Morusin on apoptosis in HCT116 and SW480 cells. (**A,B**) Cell cycle analysis was conducted with propidium iodide (PI) staining by flow cytometry. Bar graphs showed quantification of cell cycle population (%) of three independent experiments. * $p < 0.05$, *** $p < 0.001$ vs. untreated control. (**C,D**) HCT116 and SW480 cells were exposed to Morusin for 24 h and subjected to Western blotting for PARP and caspase-3. Graphs stand for relative level of protein/β-Actin as means ± SD of three independent experiments. ** $p < 0.01$ and *** $p < 0.001$ versus untreated control.

3.3. Morusin Attenuated the Expression of ZNF746 and c-Myc in HCT116 and SW480 Cells

To determine the role of c-Myc and ZNF746 in Morusin induced apoptosis, Western blotting was performed in HCT116 and SW480 cells. As shown in Figure 3A,B, Morusin significantly attenuated the protein expression of c-Myc and ZNF746 in HCT116 and SW480 cells.
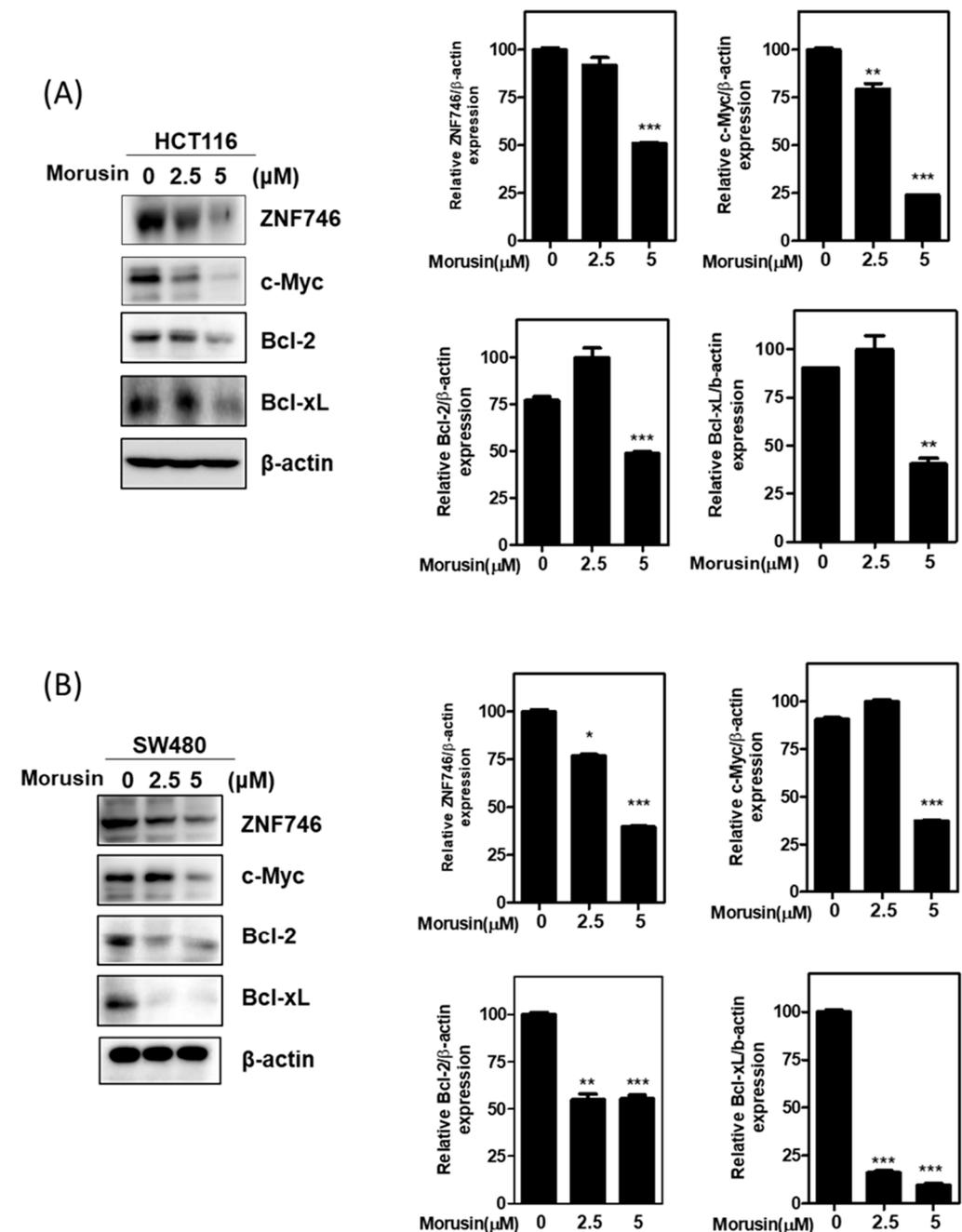
Figure 3. Effect of Morusin on the expression of ZNF746, c-Myc, Bcl-2, and Bcl-xL in HCT116 and SW480 cells. (**A**,**B**) Effect of Morusin on ZNF746, c-Myc, Bcl-2, and Bcl-xL in CRCs. HCT116 (**A**) or SW480 cells (**B**) were exposed to Morusin (0, 2.5, and 5 µM) for 24 h and subjected to Western blotting for ZNF746, c-Myc, Bcl-2, and Bcl-xL. Bar graphs stand for means ± SD for relative ZNF746, c-Myc, Bcl-2, and Bcl-xL protein expression. Data represent means ± SD of three independent experiments. * $p < 0.05$, ** $p < 0.01$ and *** $p < 0.001$ versus untreated control.

3.4. Morusin Reduced the Stability of ZNF746 and c-Myc in HCT116 and SW480 Cells in the Presence of Cycloheximide

To confirm whether Morusin regulates the stability of ZNF746 and c-Myc, a cycloheximide assay was carried out in HCT116 and SW480 cells. As shown in Figure 4A,B, Morusin reduced the half-life stability of ZNF746 and c-Myc from 15 min in HCT116 or SW480 cells exposed to DNA synthesis inhibitor cycloheximide.
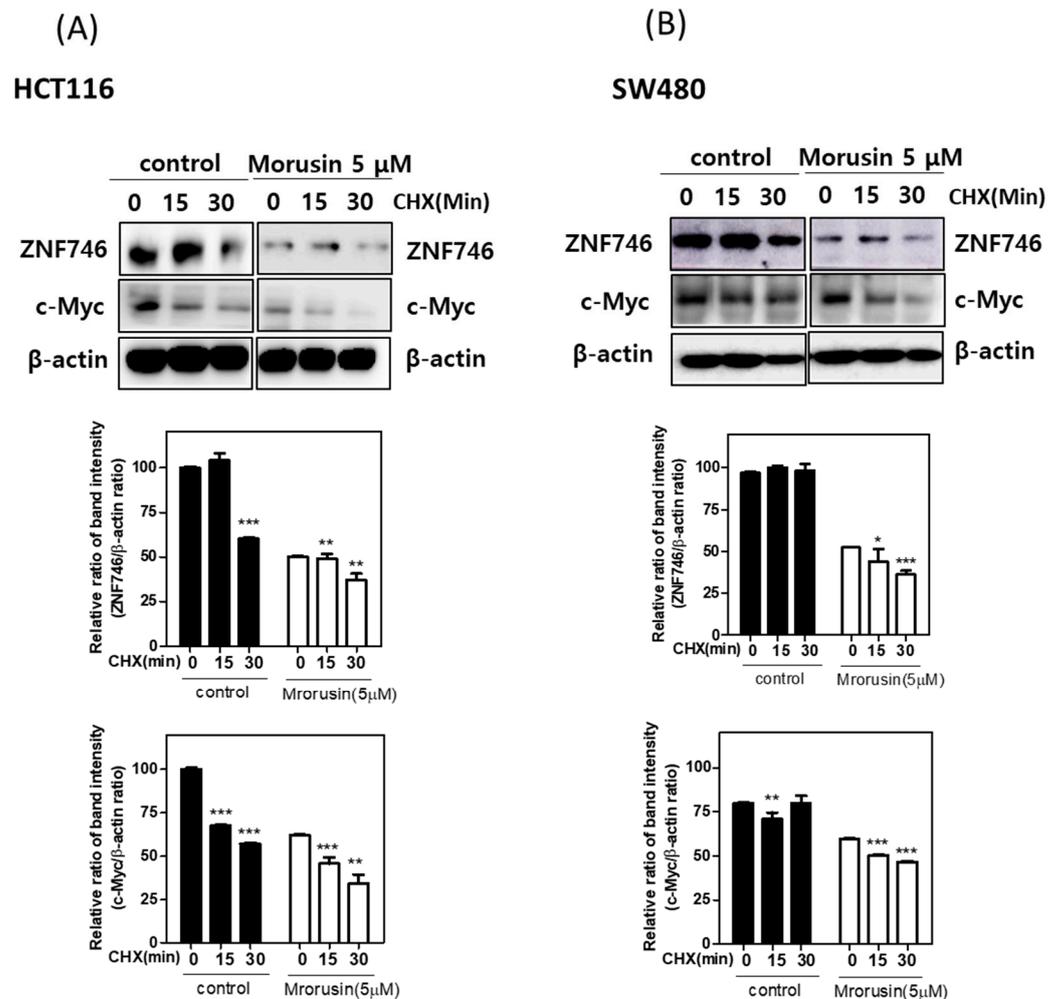
Figure 4. Effect of Morusin reduced the stability of ZNF746 and c-Myc in HCT116 and SW480 cells in the presence of cycloheximide. (**A,B**) Effect of cycloheximide on the expression of ZNF746 and c-Myc in Morusin treated HCT116 and SW480 cells. Assay was conducted in independent triplicates. * $p < 0.05$, ** $p < 0.01$ and *** $p < 0.001$ versus untreated control.

3.5. Ectopic Expression of ZNF746 Reduces Apoptotic Effect of Morusin in HCT116 Cells

To confirm the important role of ZNF746, Western blotting and TUNEL assays were carried out in HCT116 cells transfected with overexpression plasmid of ZNF746. As shown in Figure 5A,B, overexpression of ZNF746 reversed the ability of Morusin to attenuate the expression of c-Myc and ZNF746 and the number of TUNEL positive cells in HCT116 cells.

3.6. Morusin Disrupted the Binding of c-Myc and ZNF746 in HCT116 Cells

To confirm whether Morusin disrupts interaction between ZNF746 and c-Myc, immunoprecipitation was carried out in Morusin treated HCT116 cells. Here, Morusin suppressed the binding of c-Myc and ZNF746 in HCT116 cells (Figure 6A). Consistently, immunofluorescence reveals that c-Myc (red) was completely merged to ZNF746 (green) in HCT116 cells (Figure 6B).
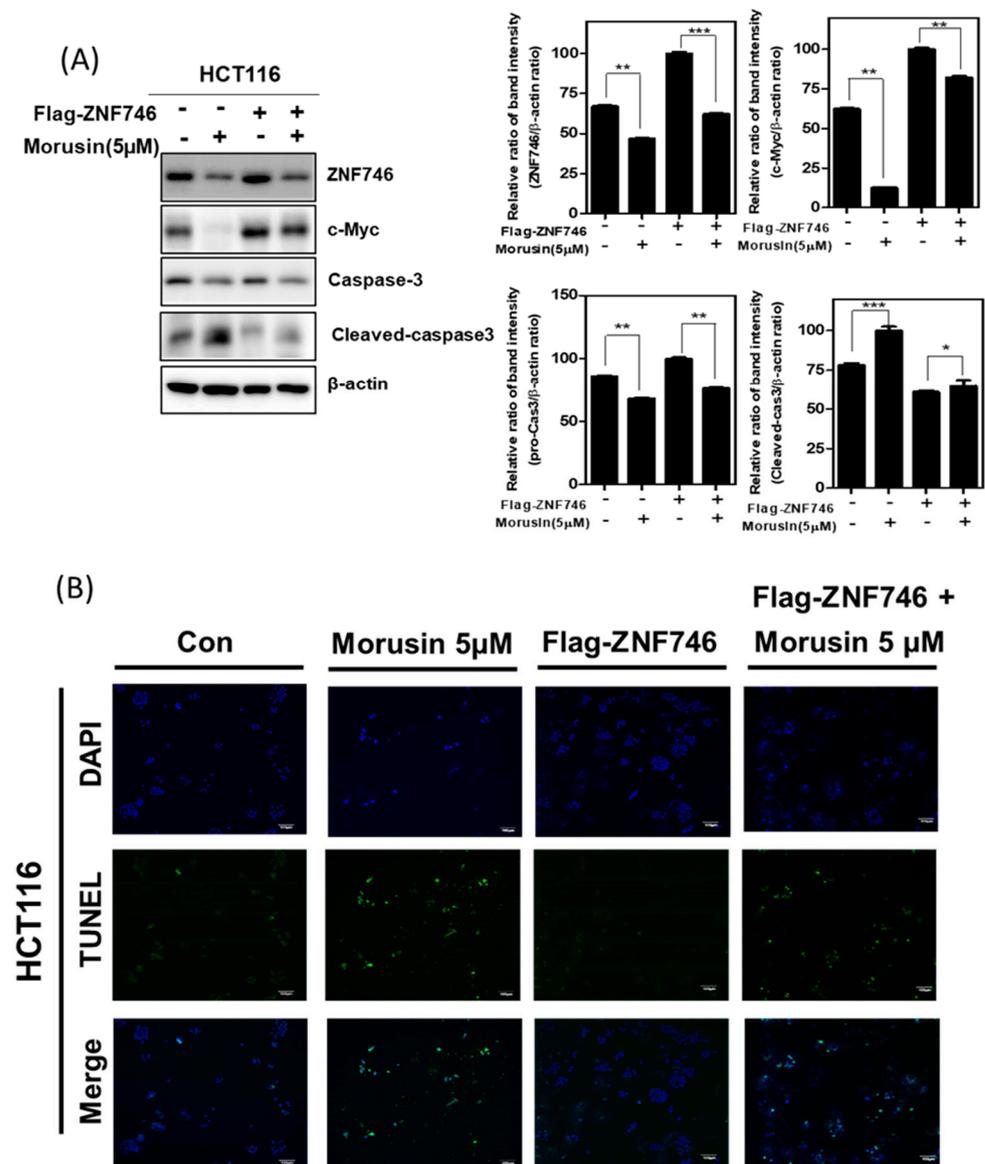
Figure 5. Ectopic expression of ZNF746 reduced apoptotic effect of Morusin in HCT116 cells. (**A**) Effect of ZNF746 overexpression on c-Myc and caspase-3 in HCT116 cells. (**B**) Effect of ZNF746 overexpression on the number of TUNEL-positive cells in HCT116 cells. The fluorescent signals from fragmented DNA (green), and DAPI (blue) by FLUOVIEW FV10i confocal microscopy. Magnification bar = 100 μM. * $p < 0.05$, ** $p < 0.01$ and *** $p < 0.001$ vs. untreated control. Assay was conducted in independent triplicates.

3.7. miR193a-5p Plays a Pivotal Role in Morusin-Induced Apoptosis in HCT116 Cells

To determine the role of miR193a-5p in Morusin-induced apoptosis, Western blotting was performed in HCT116 cells. Interestingly, TargetScan web server predicts that miR-193a-5p directly binds to the 3′-Untranslated region of c-Myc and ZNF746 by bioinformatics analysis (Figure 7A). Additionally, Morusin increased the mRNA expression of miR193a-5p in HCT116 cells (Figure 7B). Furthermore, miR193a-5p mimic reduced the expression of ZNF746, c-Myc, and pro-PARP in HCT116 cells (Figure 7C). In contrast, miR193a-5p inhibitor masked the ability of Morusin to suppress the expression of ZNF746, c-Myc, and pro-PARP in HCT116 cells (Figure 7D), implying the partial role of miR193a-5p in Morusin-induced apoptosis.

Figure 6. Effect of Morusin on interaction between c-Myc and ZNF746 in HCT116 cells by immuno-precipitation and immunofluorescence. (**A**) Effect of Morusin on the binding of c-Myc and ZNF746 in HCT116 cells by immunoprecipitation. (**B**) Effect of Morusin on the colocalization between c-Myc and ZNF746 in HCT116 cells by Immunofluorescence. Scale bars = 20 μM.

Figure 7. *Cont.*
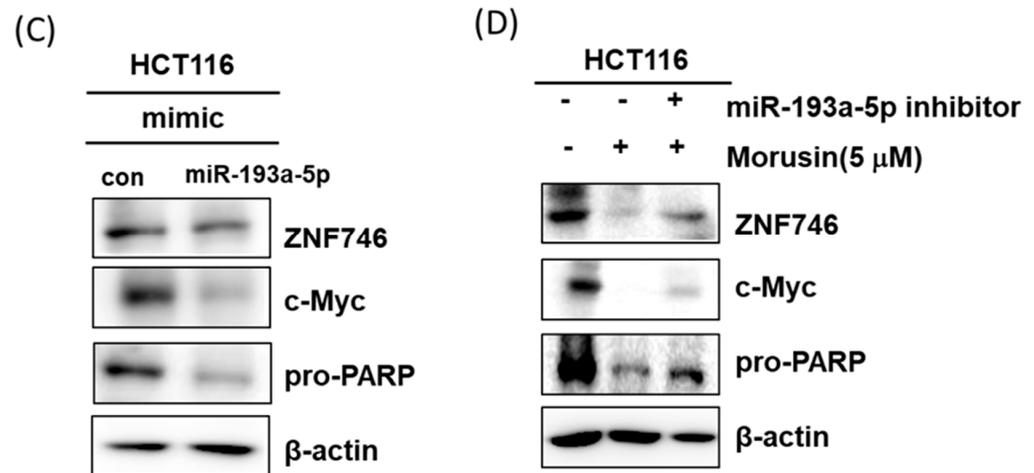
Figure 7. Effect of miR-193a-5p mimic or inhibitor in Morusin-induced apoptosis in HCT116 cells. (**A**) TargetScan web server predicts the binding sequence of miR-193a-5p in the 3′-UTR of ZNF746 and c-Myc. (**B**) Effect of Morusin on the expression of miR193a-5p in HCT116 cells by qRT-PCR. Assay was conducted in independent triplicates. ** $p < 0.01$ versus untreated control. (**C**) Effect of miR193a-5p mimic on ZNF746, c-Myc, and pro-PARP in HCT116 and cells. (**D**) Effect of miR193a-5p inhibitor on ZNF746, c-Myc, and pro-PARP in HCT116 cells.

4. Discussion

Recently, several natural compounds, including phenolic compounds, phytosterols, nitrogen compounds, carotenoids, iridoids, organosulfur compounds, essential oils, and dietary fibers [27], are gaining interest due to significant antitumor effects and low toxicity in colorectal cancers (CRCs) with combination therapy potential [28]. Though previous evidence reveals that Morusin suppresses the growth of colorectal cancer stem-like cells [3] and induces apoptosis in HT-29 CRCs via inhibition of NF-kB [29], the underlying antitumor mechanism of Morusin still remains unclear to date. Thus, in the current work, the antitumor mechanism of Morusin was investigated in association with C-Myc and ZNF746 mediated by miR193a-5p in HCT116 and SW480 cells. Herein, Morusin reduced the viability and the number of colonies in HCT116 and SW480 cells, implying the cyto-toxic and anti-proliferative effect of Morusin. It is well known that subG1 accumulation represents apoptosis in the cells [30], and cleavages of PARP and caspases indicate intrinsic or extrinsic apoptosis [31–33]. Consistently, Morusin increased sub-G1 population, and cleaved PARP and caspase-3 in HCT116 and SW480 cells, indicating the apoptotic effect of Morusin in CRCs.

Emerging evidence indicates that c-Myc is a known nuclear transcription factor oncogene among the Myc family, comprising of n-Myc, c-Myc, and l-Myc, in several cancers [34,35]. Thus, c-Myc inhibitors are considered to control tumor initiation and progression [36,37]. Additionally, ZNF746 is known to promote cancer progression via c-Myc stability in CRC [1], bladder cancer [38], and lung cancer [12]. Herein, Morusin inhibited the expression of c-Myc and ZNF746, and the stability of c-Myc, and disrupted the direct binding through nuclear colocalization in HCT116 cells. Conversely, overexpression of ZNF746 masked the antitumor effect of Morusin to reduce the expression of c-Myc and increase the number of TUNEL positive cells in HCT116 cells, demonstrating the pivotal role of C-Myc and ZNF746 in Morusin induced apoptosis.

Accumulating evidence reveals that miRNAs are critically involved in the development, cell differentiation, cell cycle, apoptosis, metastasis, and angiogenesis in several cancers as an oncogene or tumor suppressor [39,40]. Among several miRNAs, miR193a-5p is reported to inhibit liver carcinogenesis [41] and induce G1 arrest in CRCs [42]. RT-PCR reveals that Morusin upregulated miR193a-5p in HCT116 cells. As shown in bioinformatics data, miR-193a-5p directly binds to the 3′-Untranslated region of ZNF746 and c-Myc;

miR193a-5p mimic reduced the expression of ZNF746, c-Myc, and pro-PARP in HCT116 cells, while miR193a-5p inhibitor reduced the ability of Morusin to suppress the expression of ZNF746, c-Myc, and pro-PARP in HCT116 cells, indicating miR-193a-5p suppresses the expression of ZNF746, c-Myc, and pro-PARP during apoptotic effect of Morusin.

5. Conclusions

Taken together, Morusin increased cytotoxicity and sub G1 population, cleaved PARP, and attenuated the expression of pro-caspase-3 and pro-PARP in HCT116 and SW480 cells. Additionally, Morusin suppressed the expression of C-Myc and ZNF746, disturbed the binding of ZNF746 and c-Myc, and upregulated miR193a-5p in HCT116 cells. Conversely, the miR193a-5p inhibitor masked the ability of Morusin to attenuate the expression of ZNF746, c-Myc, and pro-PARP in HCT116 cells. Overall, these findings suggest that miR193a-5p mediated inhibition of C-Myc and ZNF746 signaling plays a pivotal role in Morusin induced apoptosis in CRCs (Figure 8).
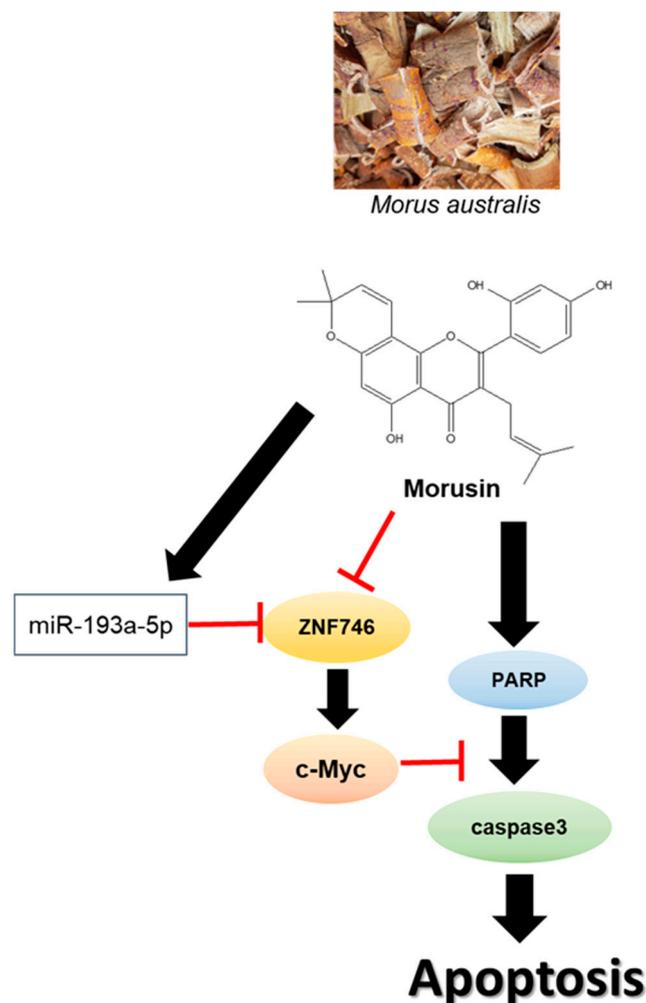
Figure 8. Schematic diagram on the apoptotic mechanism of Morusin via miR193a-5p mediated inhibition of C-Myc and ZNF746 signaling in CRCs.

Author Contributions: W.-Y.P. and H.-J.L. designed and performed the experiments; D.-Y.S., E.I., C.-H.A., and J.-E.P. analyzed the data; W.-Y.P. contributed reagents/materials/analysis tools; and B.-S.S. and S.-H.K. wrote the paper and supervised this experiment. All authors have read and agreed to the published version of the manuscript.

Institutional Review Board Statement: Not applicable.

Informed Consent Statement: Not applicable.

Conflicts of Interest: The authors declare no conflict of interest.

References

1. Jung, J.H.; Jung, D.-B.; Kim, H.; Lee, H.; Kang, S.-E.; Srivastava, S.K.; Yun, M.; Kim, S.-H. Zinc finger protein 746 promotes colorectal cancer progression via c-Myc stability mediated by glycogen synthase kinase 3β and F-box and WD repeat domain-containing 7. *Oncogene* **2018**, *37*, 3715–3728. [CrossRef]
2. Thanikachalam, K.; Khan, G. Colorectal Cancer and Nutrition. *Nutrients* **2019**, *11*, 164. [CrossRef]
3. Zhou, Y.; Li, X.; Ye, M. Morusin inhibits the growth of human colorectal cancer HCT116-derived sphere-forming cells via the inactivation of Akt pathway. *Int. J. Mol. Med.* **2021**, *47*, 1. [CrossRef]
4. Piawah, S.; Venook, A.P. Targeted therapy for colorectal cancer metastases: A review of current methods of molecularly targeted therapy and the use of tumor biomarkers in the treatment of metastatic colorectal cancer. *Cancer* **2019**, *125*, 4139–4147. [CrossRef]
5. Yiu, A.J.; Yiu, C.Y. Biomarkers in Colorectal Cancer. *Anticancer Res.* **2016**, *36*, 1093–1102.
6. Park, J.E.; Jung, J.H.; Lee, H.; Sim, D.Y.; Im, E.; Park, W.Y.; Shim, B.S.; Ko, S.; Kim, S. Ribosomal protein L5 mediated inhibition of c-Myc is critically involved in sanggenon G induced apoptosis in non-small lung cancer cells. *Phytother. Res.* **2021**, *35*, 1080–1088. [CrossRef] [PubMed]
7. Zhang, J.; Ren, P.; Xu, D.; Liu, X.; Liu, Z.; Zhang, C.; Li, Y.; Wang, L.; Du, X.; Xing, B. Human UTP14a promotes colorectal cancer progression by forming a positive regulation loop with c-Myc. *Cancer Lett.* **2019**, *440–441*, 106–115. [CrossRef]
8. Huang, J.; Wang, J.-F.; Zhang, H.-S. Structure and function of plant C2H2 zinc finger protein. *Yi Chuan* **2004**, *26*, 414–418. [PubMed]
9. Han, G.; Lu, C.; Guo, J.; Qiao, Z.; Sui, N.; Qiu, N.; Wang, B. C2H2 Zinc Finger Proteins: Master Regulators of Abiotic Stress Responses in Plants. *Front. Plant Sci.* **2020**, *11*, 115. [CrossRef]
10. Kamitani, S.; Togi, S.; Ikeda, O.; Nakasuji, M.; Sakauchi, A.; Sekine, Y.; Muromoto, R.; Oritani, K.; Matsuda, T. Krüppel-Associated Box-Associated Protein 1 Negatively Regulates TNF-α–Induced NF-κB Transcriptional Activity by Influencing the Interactions among STAT3, p300, and NF-κB/p65. *J. Immunol.* **2011**, *187*, 2476–2483. [CrossRef]
11. Cesaro, E.; Sodaro, G.; Montano, G.; Grosso, M.; Lupo, A.; Costanzo, P. The Complex Role of the ZNF224 Transcription Factor in Cancer. *Protein-Protein Interact. Hum. Dis. Part A* **2017**, *107*, 191–222. [CrossRef]
12. Kim, S.; Sohn, E.J.; Jung, J.H.; Shin, E.A.; You, O.H.; Im, J. Inhibition of ZNF746 suppresses invasion and epithelial to mesenchymal transition in H460 non-small cell lung cancer cells. *Oncol. Rep.* **2013**, *31*, 73–78. [CrossRef] [PubMed]
13. Kane, L.A.; Lazarou, M.; Fogel, A.I.; Li, Y.; Yamano, K.; Sarraf, S.; Banerjee, S.; Youle, R.J. PINK1 phosphorylates ubiquitin to activate Parkin E3 ubiquitin ligase activity. *J. Cell Biol.* **2014**, *205*, 143–153. [CrossRef]
14. Lee, Y.S.; Dutta, A. MicroRNAs in Cancer. *Annu. Rev. Pathol. Mech. Dis.* **2009**, *4*, 199–227. [CrossRef]
15. Goodall, G.J.; Wickramasinghe, V.O. RNA in cancer. *Nat. Rev. Cancer* **2021**, *21*, 22–36. [CrossRef]
16. Toden, S.; Zumwalt, T.J.; Goel, A. Non-coding RNAs and potential therapeutic targeting in cancer. *Biochim. Biophys. Acta (BBA)-Bioenerg.* **2021**, *1875*, 188491. [CrossRef]
17. Yang, Y.; Wang, T.; Chen, D.; Ma, Q.; Zheng, Y.; Liao, S.; Wang, Y.; Zhang, J. Quercetin preferentially induces apoptosis in KRAS-mutant colorectal cancer cells via JNK signaling pathways. *Cell Biol. Int.* **2019**, *43*, 117–124. [CrossRef]
18. Shan, J.; Xuan, Y.; Zhang, Q.; Zhu, C.; Liu, Z.; Zhang, S. Ursolic acid synergistically enhances the therapeutic effects of oxaliplatin in colorectal cancer. *Protein Cell* **2016**, *7*, 571–585. [CrossRef]
19. Pricci, M.; Girardi, B.; Giorgio, F.; Losurdo, G.; Ierardi, E.; Di Leo, A. Curcumin and Colorectal Cancer: From Basic to Clinical Evidences. *Int. J. Mol. Sci.* **2020**, *21*, 2364. [CrossRef]
20. Hazafa, A.; Rehman, K.-U.; Jahan, N.; Jabeen, Z. The Role of Polyphenol (Flavonoids) Compounds in the Treatment of Cancer Cells. *Nutr. Cancer* **2020**, *72*, 386–397. [CrossRef]
21. Venturelli, S.; Burkard, M.; Biendl, M.; Lauer, U.M.; Frank, J.; Busch, C. Prenylated chalcones and flavonoids for the prevention and treatment of cancer. *Nutrition* **2016**, *32*, 1171–1178. [CrossRef]
22. Dat, N.T.; Binh, P.T.X.; Quynh, L.T.P.; Van Minh, C.; Huong, H.T.; Lee, J.J. Cytotoxic prenylated flavonoids from Morus alba. *Fitoterapia* **2010**, *81*, 1224–1227. [CrossRef]
23. Wu, S.-C.; Han, F.; Song, M.-R.; Chen, S.; Li, Q.; Zhang, Q.; Zhu, K.; Shen, J.-Z. Natural Flavones fromMorus albaagainst Methicillin-ResistantStaphylococcus aureusvia Targeting the Proton Motive Force and Membrane Permeability. *J. Agric. Food Chem.* **2019**, *67*, 10222–10234. [CrossRef]
24. Jia, Y.; He, W.; Zhang, H.; He, L.; Wang, Y.; Zhang, T.; Peng, J.; Sun, P.; Qian, Y. Morusin Ameliorates IL-1β-Induced Chondrocyte Inflammation and Osteoarthritis via NF-κB Signal Pathway. *Drug Des. Dev. Ther.* **2020**, *14*, 1227–1240. [CrossRef]

25. Yang, C.; Luo, J.; Luo, X.; Jia, W.; Fang, Z.; Yi, S.; Li, L. Morusin exerts anti-cancer activity in renal cell carcinoma by disturbing MAPK signaling pathways. *Ann. Transl. Med.* **2020**, *8*, 327. [CrossRef]

26. Huang, C.-C.; Wang, P.-H.; Lu, Y.-T.; Yang, J.-S.; Yang, S.-F.; Ho, Y.-T.; Lin, C.-W.; Hsin, C.-H. Morusin Suppresses Cancer Cell Invasion and MMP-2 Expression through ERK Signaling in Human Nasopharyngeal Carcinoma. *Molecules* **2020**, *25*, 4851. [CrossRef]

27. Costea, T.; Hudiță, A.; Ciolac, O.-A.; Gălățeanu, B.; Ginghină, O.; Costache, M.; Ganea, C.; Mocanu, M.-M. Chemoprevention of Colorectal Cancer by Dietary Compounds. *Int. J. Mol. Sci.* **2018**, *19*, 3787. [CrossRef] [PubMed]

28. Rejhová, A.; Opattová, A.; Čumová, A.; Slíva, D.; Vodička, P. Natural compounds and combination therapy in colorectal cancer treatment. *Eur. J. Med. Chem.* **2018**, *144*, 582–594. [CrossRef]

29. Lee, J.-C.; Won, S.-J.; Chao, C.-L.; Wu, F.-L.; Liu, H.-S.; Ling, P.; Lin, C.-N.; Su, C.-L. Morusin induces apoptosis and suppresses NF-κB activity in human colorectal cancer HT-29 cells. *Biochem. Biophys. Res. Commun.* **2008**, *372*, 236–242. [CrossRef]

30. Kajstura, M.; Halicka, H.D.; Pryjma, J.; Darzynkiewicz, Z. Discontinuous fragmentation of nuclear DNA during apoptosis revealed by discrete "sub-G1" peaks on DNA content histograms. *Cytom. Part A* **2007**, *71*, 125–131. [CrossRef]

31. Porter, A.G.; Jänicke, R.U. Emerging roles of caspase-3 in apoptosis. *Cell Death Differ.* **1999**, *6*, 99–104. [CrossRef] [PubMed]

32. Larsen, B.; Sørensen, C.S. The caspase-activated DN ase: Apoptosis and beyond. *FEBS J.* **2017**, *284*, 1160–1170. [CrossRef] [PubMed]

33. Van Opdenbosch, N.; Lamkanfi, M. Caspases in Cell Death, Inflammation, and Disease. *Immunity* **2019**, *50*, 1352–1364. [CrossRef]

34. Elbadawy, M.; Usui, T.; Yamawaki, H.; Sasaki, K. Emerging Roles of C-Myc in Cancer Stem Cell-Related Signaling and Resistance to Cancer Chemotherapy: A Potential Therapeutic Target Against Colorectal Cancer. *Int. J. Mol. Sci.* **2019**, *20*, 2340. [CrossRef]

35. Pérez-Sayáns, M.; Suárez-Peñaranda, J.M.; Pilar, G.-D.; Barros, F.; Gándara-Rey, J.M.; Garcia-Garcia, A. What real influence does the proto-oncogene c-Myc have in OSCC behavior? *Oral Oncol.* **2011**, *47*, 688–692. [CrossRef] [PubMed]

36. Dang, C.V. MYC on the Path to Cancer. *Cell* **2012**, *149*, 22–35. [CrossRef] [PubMed]

37. Wu, H.; Yang, T.; Li, Y.; Ye, W.; Liu, F.; He, X.; Wang, J.; Gan, W.; Li, X.; Zhang, S.; et al. Tumor Necrosis Factor Receptor–Associated Factor 6 Promotes Hepatocarcinogenesis by Interacting With Histone Deacetylase 3 to Enhance c-Myc Gene Expression and Protein Stability. *Hepatology* **2020**, *71*, 148–163. [CrossRef]

38. Chen, Y.-T.; Yang, C.-C.; Shao, P.-L.; Huang, C.-R.; Yip, H.-K. Melatonin-mediated downregulation of ZNF746 suppresses bladder tumorigenesis mainly through inhibiting the AKT-MMP-9 signaling pathway. *J. Pineal Res.* **2018**, *66*, e12536. [CrossRef]

39. Tutar, Y. Editorial (Thematic Issue: "miRNA and Cancer; Computational and Experimental Approaches"). *Curr. Pharm. Biotechnol.* **2014**, *15*, 429. [CrossRef] [PubMed]

40. Rupaimoole, R.; Slack, F.J. MicroRNA therapeutics: Towards a new era for the management of cancer and other diseases. *Nat. Rev. Drug Discov.* **2017**, *16*, 203–222. [CrossRef]

41. Roy, S.; Hooiveld, G.; Seehawer, M.; Caruso, S.; Heinzmann, F.; Schneider, A.T.; Frank, A.K.; Cardenas, D.V.; Sonntag, R.; Luedde, M.; et al. microRNA 193a-5p Regulates Levels of Nucleolar- and Spindle-Associated Protein 1 to Suppress Hepatocarcinogenesis. *Gastroenterology* **2018**, *155*, 1951–1966.e26. [CrossRef]

42. Noorolyai, S.; Baghbani, E.; Maleki, L.A.; Kojabad, A.B.; Shanehbandi, D.; Shahgoli, V.K.; Mokhtarzadeh, A.; Baradaran, B. Restoration of miR-193a-5p and miR-146 a-5p Expression Induces G1 Arrest in Colorectal Cancer through Targeting of MDM2/p53. *Adv. Pharm. Bull.* **2019**, *10*, 130–134. [CrossRef] [PubMed]